DOI:10.12119/j.yhyj.201902006

Isothermal Evaporating Phase Equilibria in the Quaternary System ($LiCl + NaCl + Li_2SO_4 + Na_2SO_4 + H_2O$) at 348.15 K and 0.1 MPa: An Experimental and Theoretical Study

GUO Ya-fei[1,2], YUAN Fei[1], LI Long[1], WANG Shi-qiang[1,2], DENG Tian-long[1,2]

(1. *College of Marine and Environmental Sciences, Tianjin University of Science and Technology, Tianjin*, 300457, *China*; 2. *Tianjin Key Laboratory of Marine Resources and Chemistry, Tianjin*, 300457, *China*)

Abstract: The gradient solar pond technique is an economic separating process employed in the inorganic chemical industrial production of salt lake chemical engineering processes. In this paper, a novel isothermal evaporation experimental method was employed to simulate the evaporation phase equilibrium for the reciprocal quaternary system ($LiCl + NaCl + Li_2SO_4 + Na_2SO_4 + H_2O$) at 348.15 K to serve as a useful guide for lithium salt production via the depth solar ponds. The isothermal evaporation equilibrium solubilities and physicochemical properties, including the densities and pH values, were experimentally investigated. The dry-salt phase diagram, water-phase diagram, and the diagram of the physicochemical properties versus composition were plotted with respect to the experimental data. The dry-salt phase diagram consists of three invariant points, seven univariant solubility curves, and five crystallization regions, specifically halite (NaCl, Ha), thenardite (Na_2SO_4, Th), double salt ($Li_2SO_4 \cdot Na_2SO_4$, Db_2), lithium sulfate monohydrate ($Li_2SO_4 \cdot H_2O$, Ls), and lithium chloride monohydrate ($LiCl \cdot H_2O$, Lc). Based on Pitzer and its extended HMW model, the Pitzer single salt parameters, mixing ion interaction parameters, and thermodynamic stable equilibrium constants for the quaternary system at 348.15 K were obtained. The calculated phase diagram and experimental isothermal phase diagram at 348.15 K exhibited a great difference. Based on these results, the isothermal evaporation phase diagram can truly reflect the salt sedimentary in salt lakes and can be applied as a useful guide for the solar pond process.

Key words: Phase diagram; Solubility; Lithium chloride; Lithium sulfate; Pitzer model

CLC number: O642.42 **Document code**: A **Article ID**: 1008 - 858X(2019)02 - 0069 - 09

1 Introduction

Although oceans contain an estimated amount of 2×10^{12} t of lithium resources, its low concentration ($0.17\ mg \cdot dm^{-3}$) precludes its use as lithium resource[1]. At present, almost 83% of lithium is obtained from salt lake brines by applying the evapora-

Received date: 2019 - 03 - 29; **Revised date**: 2019 - 04 - 09

Fund projects: National Natural Science Foundation of China (U1607123, 21773170 and U1707602), the Key Projects of Natural Science Foundation of Tianjin (18JCZDJC10040) and the Yangtze Scholars and Innovative Research Team of the Chinese University (IRT_17R81)

First and corresponding author: GUO Ya - fei (1981 -), female, senior engineer, mainly engaged in the study of solution chemistry. Email: guoyafei@tust.edu.cn.

tion process in brine sources in Bolivia, Chile, Argentina, and China[2]. In particular, the Qinghai-Tibet Plateau in China has more than 700 salt lakes with an area larger than 1 km^2[3]. The composition of salt lake brines is mainly composed of the complex seven-component system of $Li^+ + Na^+ + K^+ + Mg^{2+} + Cl^- + SO_4^{2-}$ + borate + H_2O[4]. Although brine resources are very valuable, the development and utilization has not been reported due to a lack of relative solubilities and phase diagrams on the relative brine system.

The salt lakes around the world are windy, have weather aridity, exhibit little rainfall, and have great evaporation capacities. Lithium resources must adequately adopt the local natural resources of salt lake regions such as the solar energy resources for the solar pond technique. Therefore, isothermal evaporation phase equilibrium is essential to either predict the crystallized path or guide the industrial production of salt lake chemical engineering. In addition, the temperature in the troposphere layer of a 5 – meter-deep solar pond is as high as about 348 K, thus requiring the isothermal evaporation phase equilibrium of this system ($LiCl + NaCl + Li_2SO_4 + Na_2SO_4 + H_2O$) at 348.15 K to separate valuable lithium salt products.

Although the thermodynamic stable phaseequilibrium at 273.15, 298.15, and 323.15 K[5,6] for the quaternary system ($LiCl + NaCl + Li_2SO_4 + Na_2SO_4 + H_2O$) has been reported in the literature, the isothermal evaporation phase diagram for this reciprocal quaternary system at 348.15 K has not been reported.

Because the solubilities of lithium salts in the salt-water system generally have high molality, it is necessary to use a reliable theory for aqueous electrolyte solutions to calculate their respective solubilities. On the basis of Pitzer's ion interaction theory[7,8], Harvie, Møller, and Wear developed a chemical equilibrium horizontal wind model (HWM)[9-13], which was successfully utilized in natural waters of high ionic strength (Harvie *et al.*, 1980; Harvie and Weare, 1980; Felmy and Weare, 1986). Song[14] and Fang *et al.*[15] applied the HWM model to calculate the isothermal evaporation phase equilibria of salt-water systems. Previous studies on the quaternary system ($LiCl + NaCl + Li_2SO_4 + Na_2SO_4 + H_2O$) at 348.15 K have rarely reported upon the Pitzer single-salt and mixing ion interaction parameters of LiCl, NaCl, Li_2SO_4, and Na_2SO_4 as well as the isothermal evaporation mineral equilibrium constants of NaCl, Na_2SO_4, $Li_2SO_4 \cdot Na_2SO_4$, $Li_2SO_4 \cdot H_2O$, and $LiCl \cdot H_2O$, especially for the lithium-containing minerals at 348.15 K at wide concentration ranges.

In this paper, theisothermal evaporation solubility and physicochemical property data of the quaternary system at 348.15 K were measured. The theoretic predictive solubilities were carried out on the basis of Pitzer and its extended HMW model.

2 Experimental Section

2.1 Apparatus and reagents

The isothermal evaporation chamber was temperature and humidity controlled (LHS – 250HC – I, Chinese Yihen Scientific Instruments Co. Ltd.) with the precisions of ±0.1 K and humidity values within ±0.5%. The solid phase minerals that were identified were combined with a digital polarizing microscope (BX51 – P, Olympus, Japan) and an X-ray diffractometer (X'pertPRO, Spectris. Pty. Ltd., The Netherlands).

The chemicals were recrystallized before use. The chemical sample descriptions are shown in Table 1. Doubly deionized water (DDW) with a conductivity of less than 1×10^{-4} $S \cdot m^{-1}$ at room temperature was used to prepare the series of artificially synthesized brines and for chemical analysis.

Table 1 Chemicals used in this study

Code	Grade	Initial mass fraction purity	Purification method	Final mass fraction purity	Analysis method
Ha	A. R. [a]	0.99	Re-crystallization	0.995	Titration of Cl^-
Lc	A. R. [a]	0.99	Re-crystallization	0.995	
Th	A. R. [b]	0.99	Re-crystallization	0.995	Gravimetric
Ls	A. R. [d]	0.99	Re-crystallization	0.995	method for SO_4^{2-}

Ha, sodium chloride (NaCl), from the Sinopharm Chemical Reagent Co., Ltd.

Lc, lithium chloride monohydrate ($LiCl \cdot H_2O$), from Xinjiang Nonferrous Metal Industry Co. Ltd.

Th, sodium sulfate (Na_2SO_4), from Tianjin Guangfu Technology Development Co. Ltd.

Ls, lithium sulfate monohydrate ($Li_2SO_4 \cdot H_2O$), from Shanghai Lithium Industrial Co. Ltd.

2.2 Experimental methods

The present study applied the isothermal evaporation method. A series of synthetic brine were loaded in each clean polyethylene container, which had diameters of 15 cm and depths of 6 cm. The containers were then placed in an isothermal evaporation chamber at 348.15 ± 0.1 K. The experimental conditions were similar to the climate of salt lakes with a relative humidity of 25% ± 0.5%. The solutions were not stirred during isothermal evaporation, and the crystal behavior of the solid phase was periodically observed though the window of the chamber. When enough new solid phases were observed, specifically about 0.5 ~ 1.0 g, the wet residue mixtures were removed from the solution. The solids were then evaluated with combined chemical analysis using digital polarizing microscopy and further identified via X-ray diffraction. Meanwhile, a 5 cm^3 sample of the clear liquid phase solution was removed from the liquid phase of each polyethylene container using the pipettor. The samples were diluted to 250 mL in a volumetric flask with DDW for the quantitative analysis of the liquid phase compositions. Another aliquot of the clear liquid phase solution was used to measure the individual relative physicochemical properties of the samples, specifically the density and pH values. The rest of the solution was allowed to evaporate to reach a new isothermal evaporation equilibrium point.

2.3 Analytical methods

The concentrations of the SO_4^{2-} ion in the liquid phase were analyzed by gravimetric methods using barium chloride as the precipitator with a mass fraction uncertainty within 0.000 5. The Cl^- ion concentration was determined by titration with a mercury nitrate standard solution in the presence of a mixed indicator, specifically diphenylcarbazone and bromophenol blue, with a mass fraction uncertainty of ± 0.003. The Li^+ ion concentration was evaluated using an ion balance combined with analytical verification using ICP-OES (inductively coupled plasma optical emission spectrometry; Prodigy, Leman Corporation, USA) with an uncertainty of ±0.005[16].

A high precision pH meter (PHSJ - 5, supplied by the Shanghai Precision Scientific Instrument Co. Ltd., China) was used to measure the pH of the equilibrium aqueous solutions with an uncertainty of less than ±0.003. The pH meter was calibrated using the two standard buffer solutions of potassium dihydrogen phosphate and disodium hydrogen phosphate (pH 6.980) and borax (pH 9.460). The density (ρ) was measured using an Anton Paar Digital vibrating tube densimeter (DMA 4500, Anton Paar Co. Ltd., Austria) with an uncertainty of less than ±0.5 $mg \cdot cm^{-3}$. All the measurements were maintained at the desired temperature of 348.15 ± 0.1 K by controlling the thermostat.

3 Results and Discussion

The isothermal evaporating solubilities and physicochemical properties, including the density and pH value of the quaternary system ($LiCl + NaCl + Li_2SO_4 + Na_2SO_4 + H_2O$) at 348.15 K, were measured and are shown in Table 2.

Table 2 Solubility dates and physicochemical property dates of the isothermal evaporating equilibrium quaternary system (Li^+, $Na^+//Cl^-$, $SO_4^{2-} - H_2O$) at $T = 348.15$ K and p = 0.1 MPa[a]

No.	Composition of liquid phase100w[b]				Janecke index J_b, /[mol/100 mol($2Li^+ + 2Na^+$ = 100 mol)]			pH	ρ, /($g \cdot cm^{-3}$)	Equilibrium solide phase[c]
	Li^+	Na^+	Cl^-	SO_4^{2-}	$2Na^+$	SO_4^{2-}	H_2O			
1, A	0.00	10.43	13.80	3.09	100.00	14.19	1 772.38	5.821	1.232 5	Th + Ha
2	0.53	10.17	15.13	4.41	85.27	17.70	1 488.25	7.490	1.265 3	Th + Ha
3	0.69	9.62	15.04	4.50	80.81	18.10	1 498.30	7.294	–	Th + Ha
4, E_1	1.06	8.61	14.99	5.03	70.99	19.87	1 474.26	7.299	1.262 8	Th + Ha + Db2
5	1.22	8.07	15.34	4.48	66.71	17.73	1 490.73	–[d]	1.200 1	Ha + Db2
6	1.17	8.18	14.76	5.17	67.92	20.54	1 493.30	7.399	–	Ha + Db2
7	1.47	7.19	15.84	3.74	59.62	14.82	1 512.91	7.332	1.190 6	Ha + Db2
8	1.51	7.07	16.07	3.44	58.64	13.64	1 515.92	7.226	1.186 5	Ha + Db2
9	1.88	6.80	18.00	2.84	52.21	10.43	1 375.59	–	–	Ha + Db2
10	2.44	4.40	17.21	2.76	35.29	10.57	1 491.09	7.296	1.166 5	Ha + Db2
11	2.60	4.09	17.74	2.50	32.19	9.41	1 463.13	7.163	1.168 7	Ha + Db2
12	2.80	3.68	18.31	2.26	28.38	8.36	1 431.35	6.650	1.164 3	Ha + Db2
13	2.98	3.27	18.76	2.03	24.90	7.40	1 412.47	–	–	Ha + Db2
14	3.11	3.00	19.05	1.96	22.59	7.06	1 394.59	6.343	–	Ha + Db2
15, E_2	3.17	2.75	19.04	1.88	20.80	6.79	1 404.98	6.021	1.157 2	Ha + Db2 + Ls
16	3.63	1.70	20.47	0.97	12.41	3.39	1 355.62	4.280	1.156 6	Ha + Ls
17	3.70	1.63	20.72	0.96	11.74	3.31	1 335.48	–	–	Ha + Ls
18, E_3	8.37	0.16	42.93	0.089	0.57	0.15	441.93	2.380	1.345 2	Ha + Ls + Lc
19, B	1.13	8.67	0.00	25.96	69.88	100.00	1 314.80	8.277	1.320 8	Th + Db2
20	1.08	7.87	6.55	15.01	68.82	62.84	1 546.12	–	–	Th + Db2
21	1.03	7.93	10.69	9.21	69.92	38.86	1 595.52	–	1.331 2	Th + Db2
22	0.99	8.27	12.18	7.62	71.60	31.60	1 562.87	–	–	Th + Db2
23, C	2.71	2.93	0.00	24.89	24.66	100.00	1 482.97	8.072	1.279 6	Ls + Db2
24	2.67	2.28	7.39	13.20	20.51	56.86	1 703.43	7.539	1.188 1	Ls + Db2
25	2.62	2.31	8.32	11.69	21.02	50.91	1 736.44	7.539	1.188 1	Ls + Db2
26	2.78	2.33	13.87	5.34	20.15	22.12	1 666.32	7.529	1.180 1	Ls + Db2
27, D	8.61	0.00	43.94	0.031	0.00	0.051	423.08	7.070	–	Ls + Lc
28, F	6.19	0.14	31.82	0.00	0.69	0.00	762.12	4.750	1.336	Ha + Lc

[a]Standard uncertainties u are $u(T) = 0.1$ K, $u(p) = 0.005$ MPa. u(x) for Li_2SO_4, Na_2SO_4, LiCl and NaCl are 0.000 57, 0.000 74, 0.003 58 and 0.004 94 in mass fraction, respectively. $u(x)$ for ρ and pH are 0.5 mg cm^3 and 0.003, respectively.

[b]w, mass fraction.

[c]Th, Na_2SO_4; Ha, NaCl; Db2, $Li_2SO_4 \cdot NaSO_4$; Ls, $Li_2SO_4 \cdot H_2O$; Lc, $LiCl \cdot H_2O$;

[d] –, not determined.

On the basis of the Janecke index (J, [mol/100 mol ($2\ Na^+ + 2\ Li^+$)]) in Table 2, the isothermal evaporation equilibrium phase diagram of the system at 348.15 K was plotted (Fig. 1). In Fig. 1, the isothermal evaporating phase diagram consists of three invariant points, seven univariant curves, and five crystallization regions corresponding to halite (NaCl, Ha), thenardite (Na_2SO_4, Th), double salt ($Li_2SO_4 \cdot Na_2SO_4$, Db2), lithium sulfate monohydrate ($Li_2SO_4 \cdot H_2O$, Ls), and lithium chloride monohydrate ($LiCl \cdot H_2O$, Lc). The double salt Db_2 crystallized phase region exhibited the largest area, whereas the Lc crystallized region exhibited the smallest area. This result indicated the easy precipitation of the double salt Db_2, while the lithium chloride was precisely enriched in the liquid solution. No solid solution was observed except for double salt of $Li_2SO_4 \cdot Na_2SO_4$ in the isothermal evaporation equilibrium system. Fig. 2 presents the water-phase diagram of the quaternary system at 348.15 K, wherein the Janecke index of $J(H_2O)$ gradually changed with increasing $J(Na^+)$ in the solution. In addition, the water content in the co-saturated solubility curves of the two minerals of BE_1 (Ls + Db_2) and CE_2 (Db + Th) first increased and then decreased with increasing $J(2Na^+)$. Similarly, the water content in the co-saturated solubility curves of AE_1 (Ha + Th), E_1E_2 (Ha + Db_2), and E_2E_3 (Ha + Ls) always increased with increasing $J(2Na^+)$.

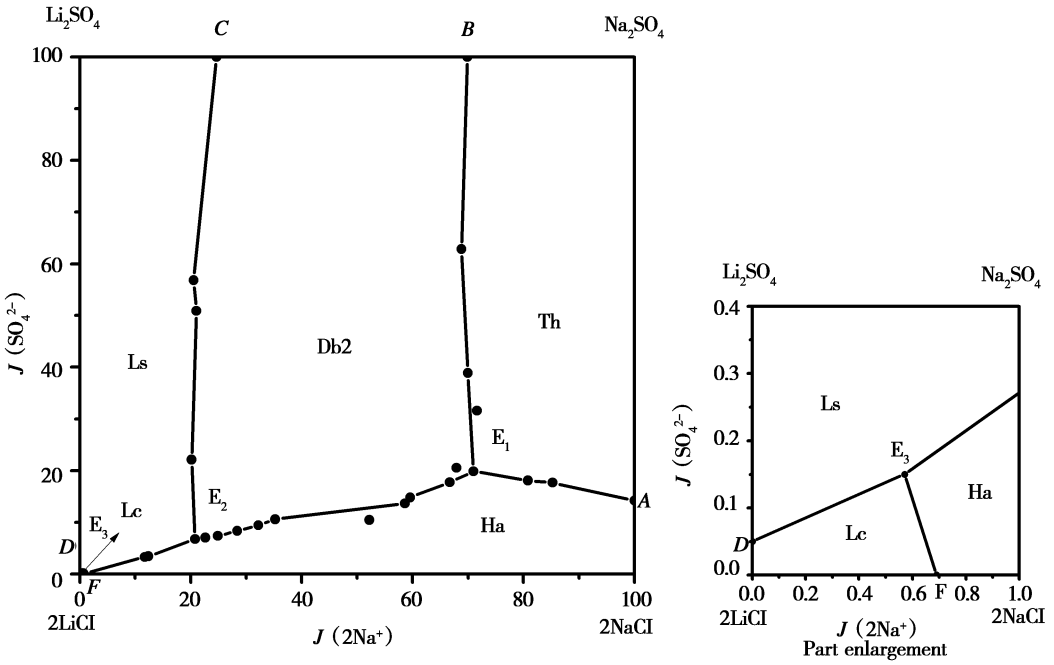

Fig. 1 Isothermal evaporating phase diagram of the quaternary system (Li^+, $Na^+//Cl^-$, SO_4^{2-} – H_2O) at 348.15 K. (●), experiment point at 348.15 K; (–) solubility curve at 348.15 K; Th, Na_2SO_4; Ha, NaCl; Db2, $Li_2SO_4 \cdot NaSO_4$; Ls, $Li_2SO_4 \cdot H_2O$; Lc, $LiCl \cdot H_2O$

According to the experimental data in Table 1, a comparison of the physicochemical properties versus the composition diagram for the isothermal evaporating quaternary system ($LiCl + NaCl + Li_2SO_4 + Na_2SO_4 + H_2O$) at 348.15 K is plotted in Fig. 3. The densities and pH values regularly changed with increasing $J(2Na^+)$ in the solution. With increasing $J(2Na^+)$, the density in the co-saturated solubility curves of the two minerals of FE_3 (Ha + Lc) and E_3E_2 (Ha + Ls) decreased, whereas the co-saturated solubility curves of E_2E_1 (Ha + Db2) and E_1A (Ha + Th) increased gradually. The densities in

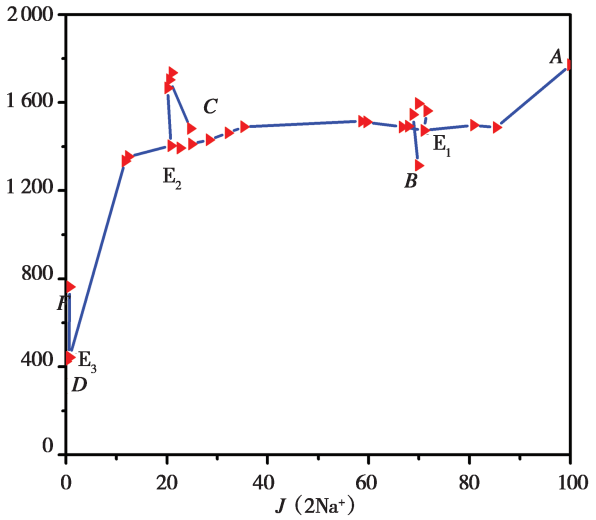

Fig. 2 Water-phase diagram of the quaternary system (Li^+, $Na^+//Cl^-$, SO_4^{2-} – H_2O) at 348.15 K. (▸), experimental point at 348.15 K; (–), solubility curve

4 Predictive solubility

4.1 Ion-interaction HMW model

Pitzer *et al*. developed an ion interaction theory and published a series of papers[7,8] that presented a set of expressions for osmotic coefficients for the solution and mean activity coefficient of electrolytes in the solution. The expressions of the chemical equilibrium model for the conventional single-ion activity coefficients derived by Harvie, Møller, and Wear[17,18] are more convenient for use in solubility calculations. The use of equilibrium solid phase activity coefficients and solubility products allowed us to identify the coexisting solid phases and their respective compositions at equilibrium. Additional work has been centered upon the development of variable-temperature models, which will increase the applicability to a number of diverse geochemical systems[11,13,19].

4.2 Model parameterization

Møller *et al*.[9,11-12,19] used an expanded model to establish the high temperature chemical model in

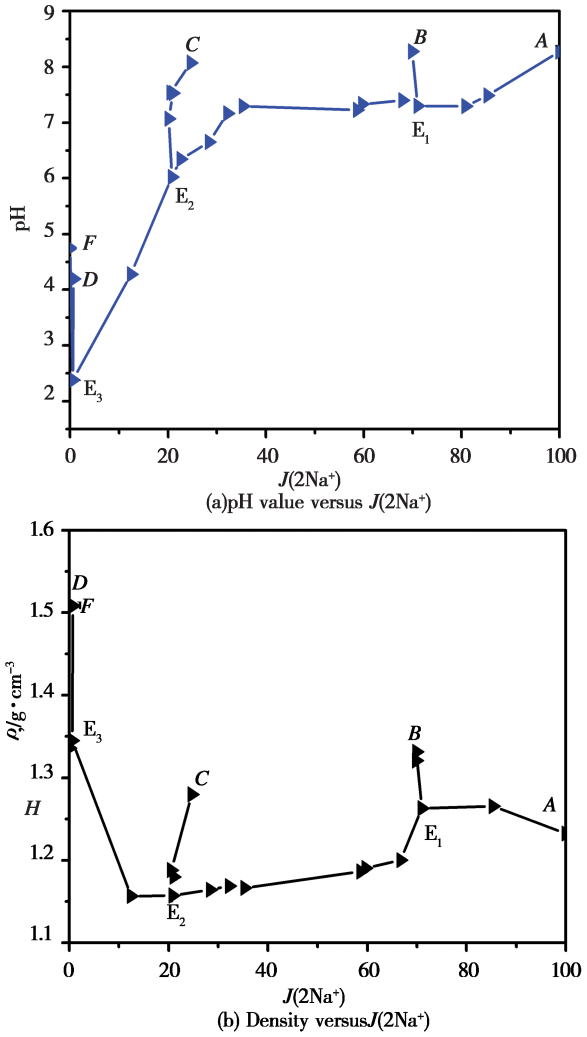

Fig. 3 Physicochemical properties-composition diagram for the isothermal evaporating equilibrium quaternary system (Li^+, $Na^+//Cl^-$, SO_4^{2-} – H_2O) at 348.15 K. (▸), experimental point at 348.15 K; (–), solubility curve. (a), pH vs. J($2Na^+$); (b), (b) density vs. J($2Na^+$)

Equation (1) to calculate mineral solubility successfully in natural waters (Na^+, K^+, $Ca^{2+}//Cl^-$, SO_4^{2-} – H_2O) and (Na^+, $Mg^{2+}//Cl^-$, SO_4^{2-}, OH^- – H_2O) and in calcium acid-base systems (H^+, Na^+, K^+, $Ca^{2+}//OH^-$, Cl^-, HSO_4^-, SO_4^{2-} – H_2O) from low to high solution concentrations within about 273.15 – 473.15 K. The Pitzer single-salt parameters of NaCl and Na_2SO_4 as well as the Pitzer mixing ion interaction parameters of $\theta_{Cl,SO4}$ and $\Psi_{Na,Cl,SO4}$ at 348.15 K in this work were obtained by following temperature-dependent Equation

(1) as presented by Greenberg[11] at a Debye-Hückel limiting slope of $A^{\Phi} = 0.433\ 30$ at 348.15 K:

$$P(T) = a_1 + a_2T + a_3/T + a_4\ln T + a_5/(T - 263) + a_6T^2 + a_7(680 - T) + a_8/(T - 227) \quad (1)$$

Variable temperature chemical models for salt-water systems containing lithium have rarely been reported. As to lithium chloride, previous studies reported the osmotic coefficients of lithium chloride aqueous solutions from 0.1 to 18.0 molalities at 273.15, 298.15, 323.15, 348.15, and 373.15 K[20]. Therefore, the osmotic coefficients of lithium chloride aqueous solutions from 0.1 to 18.0 molalities at 348.15 K may be obtained through interpolation based on presented osmotic coefficients at other temperatures. The Pitzer single-salt parameter of lithium chloride at 348.15 K was fit against attained osmotic coefficients of the aqueous lithium chloride solutions. In addition, the Pitzer single-salt parameter of lithium sulfate at 348.15 K was calculated according to the temperature-dependent, Equation (2), which was previously presented by Holmes[21]:

$$P(T) = p_1 + p_2(TR - TR^2/T) + p_3(T^2 + 2TR^3/T - 3TR^2) + p_4(T + TR^2/T - 2TR) + p_5(\ln(T/TR) + TR/T - 1) + p_6(1/(T - 263) + (263T - TR^2)/T/(TR - 263)^2) + p_7(1/(680 - T) + (TR^2 - 680T)/T/(680 - TR)^2), \quad (2)$$

where TR = 298.15 K. The mixing pair parameter $\theta_{Li,Na}$ and the mixing triplet parameter of $\Psi_{Li,Na,Cl}$ and $\Psi_{Li,Cl,SO4}$ were fitted against the equilibrium solubility data of the relative ternary systems ($LiCl + NaCl + H_2O$) and ($LiCl + Li_2SO_4 + H_2O$)[22,23]. All Pitzer signal salt parameters and mixing ion interaction parameters for the reciprocal quaternary system ($LiCl + NaCl + Li_2SO_4 + Na_2SO_4 + H_2O$) at 348.15 K are shown in Tables 3 and 4, respectively.

The equilibrium constants, K_{sp}, of five kinds of minerals in the quaternary system at 348.15 K with respect to the solubility data of the aqueous binary systems as well as the sub-ternary systems at 348.15 K and the fitted Pitzer parameters in Table 3 are listed in Table 5.

Table 3 Single salt Pitzer parameters of the quaternary system ($LiCl + NaCl + Li_2SO_4 + Na_2SO_4 + H_2O$) at 348.15 K

Single salts	Parameters			
	$\beta^{(0)}$	$\beta^{(1)}$	$\beta^{(2)}$	C^{ϕ}
LiCl	0.180 6	−0.185 1	–	−0.004 293
Li_2SO_4	0.144 1	1.334 4	–	−0.011 787
NaCl	0.096 68	0.314 5	–	−0.002 282
Na_2SO_4	0.088 86	1.288 9	–	0.005 502

Table 4 Mixing ion-interaction parameters of the quaternary system ($LiCl + NaCl + Li_2SO_4 + Na_2SO_4 + H_2O$) at 348.15 K

Parameters	Value	Parameters	Value
$\theta_{Li,Na}$	0.0201600	$\Psi_{Li,Na,Cl}$	−0.0074160
$\Theta_{Cl,SO4}$	0.0200000	$\Psi_{Li,Na,SO4}$	−0.0077740
A^{ϕ}	0.43330	$\Psi_{Na,Cl,SO4}$	−0.007416

Table 5 Values for equilibrium constant of minerals in the quatnary system ($LiCl + NaCl + Li_2SO_4 + Na_2SO_4 + H_2O$) at 348.15 K

Minerals	Abbr of minerals	$\ln K_{sp}$
NaCl	Ha	3.711 6
Na_2SO_4	Th	−0.110 5
$LiCl \cdot H_2O$	Lc	10.610 4
$Li_2SO_4 \cdot H_2O$	Ls	−0.348 2
$Li_2SO_4 \cdot Na_2SO_4$	Db2	−1.731 2

4.3 Thermodynamic stable equilibrium solubility calculation

Using the chemical equilibrium HMW model and the above parameters, thethermodynamic stable phase equilibrium solubility for this quaternary system at 348.15 K was calculated with Fortran 77 programming on the basis of the digital visual Fortran Software 5.0. The stable dry-salt phase diagram and water phase diagrams for the quaternary system at 348.15 K are plotted in Figs. 4 and 5 with the hollow garden lines.

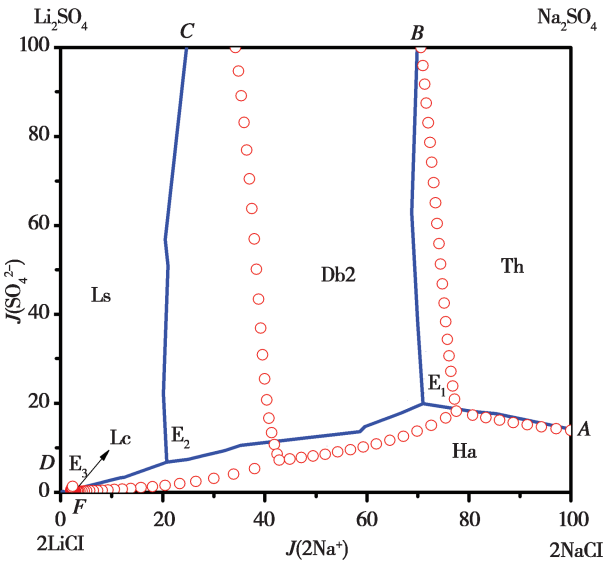

Fig. 4 Comparison of the calculated stable equilibrium and experimental isothermal evaporating phase diagram of the quaternary system (Li^+, $Na^+//Cl^-$, SO_4^{2-} – H_2O) at 348.15 K. (–), experimental curve; (○), calculate curve. Th, Na_2SO_4; Ha, NaCl; Db2, $Li_2SO_4 \cdot NaSO_4$; Ls, $Li_2SO_4 \cdot H_2O$; Lc, $LiCl \cdot H_2O$

Considering that the thermodynamic stable equilibrium solubility data have not been previously reported, the performed comparison of the isothermal evaporating phase diagram and the calculated stable phase diagram at 348.15 K indicated that (1) the calculated stable phase diagram has the same number of crystallization regions with the experimental isothermal evaporating phase diagram; (2) the compositions of the two invariant points E_1 (Ha + Ls + Db_2) and E_2 (Ha + Db_2 + Th) exhibited significant changes; and (3) the areas of crystallization of Ha (NaCl), Th (Na_2SO_4), and Db_2 ($Li_2SO_4 \cdot Na_2SO_4$) were obviously reduced, whereas Ls (Li_2SO_4) presented a markedly enlarged areas of crystallization. Based on these observations, the presented isothermal evaporating phase diagram can be used as a guideline to produce lithium sulfate from high concentration lithium-containing salt lake brine. In other words, the stable phase diagram is no longer an appropriate map for the solar pond separating process.

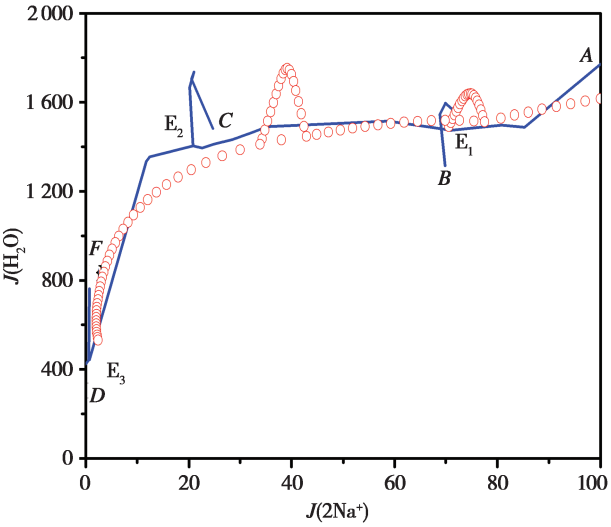

Fig. 5 Comparison of the calculated stable equilibrium and experimental isothermal evaporating equilibrium water-phase diagram of the quaternary system (Li^+, $Na^+//Cl^-$, SO_4^{2-} – H_2O) at 348.15 K; (–), experimental curve; (○), calculate curve

5 Conclusions

The present study experimentally determined the solid-liquid isothermal evaporation equilibrium solubilities and physicochemical properties of the quaternary system (LiCl + NaCl + Li_2SO_4 + Na_2SO_4 + H_2O) at 348.15 K. The isothermal evaporating equilibrium phase diagram, water-phase diagram, and the diagrams of the physicochemical properties versus composition were plotted based on the experimental data. The thermodynamic stable equilibrium solubility data were calculated according to the Pitzer single salt parameters and the mixing ion-interaction

parameters of the HWM model, upon which the equilibrium constants for this quaternary system were obtained. The calculated stable phase diagram of the quaternary system presented a great difference with the isothermal evaporating phase diagram in either of the compositions of the invariant points or the areas of the mineral crystallization regions. The isothermal evaporation phase diagram can truly reflect the salt sedimentary in the salt lakes and appears to be a more useful guide for the solar pond process in salt lake chemical engineering.

References:

[1] Vikstrom H, Davidsson S, Hook M. Lithium availability and future production outlooks [J]. Appl. Energy, 2013, 110: 252 – 266.

[2] Trocoli R, Battistel A, Mantia F L, *et al*. Nickel hexacyanoferrate as suitable alternative to Ag for electrochemical lithium recovery [J]. ChemSusChem, 2015, 8: 2514 – 2519.

[3] Guo Y F, Liu Y H, Wang Q, *et al*. Phase equilibria and phase diagram for the aqueous ternary system ($Na_2SO_4 + Li_2SO_4 + H_2O$) at (288 and 308) K [J]. J. Chem. Eng. Data, 2013, 58: 2763 – 2767.

[4] Deng T L, Guo Y F, Wang S Q. Metastable Phase Equilibria and Phase Diagrams for the salt lake brine system in Qaidam Basin [M]. Beijing: Science Press, 2017: 8 – 13.

[5] Campbell A N, Kartzmark E M, Lovering E G. Reciprocal salt pairs, involving the cations Li^+, Na^+, K^+, the anions SO_4^{2-}, Cl^- and water at 25 ℃ [J]. Can. J. Chem, 1958, 36 (1): 1511 – 1517.

[6] Hu K Y. Phase equilibria in the quaternary system $LiCl - NaCl - Li_2SO_4 - Na_2SO_4 - H_2O$ [J]. Russ. J. Inorg. Chem., 1960, 5(1): 191 – 196.

[7] Pitzer K S. Thermodynamics of Electrolyte. I. J. Phys. Chem., 1973, 77: 268 – 277.

[8] Pitzer K S. Thermodynamics: Semi-empirical equations for pure and mixed electrolytes [M]. New York: McGraw – Hill, 1995.

[9] Christov C, Moller N. A chemical equilibrium model of solution behavior and solubility in the $H - Na - K - Ca - OH - Cl - HSO_4 - SO_4 - H_2O$ system to high concentration and temperature [J]. Geochim. Cosmochim. Acta, 2004, 68(18): 1309 – 1331.

[10] Moller N, Greenberg J, Weare J. Computer modeling for geothermal systems: predicting carbonate and silica scale formation, CO_2 breakout and H_2S exchange [J]. Transport. Porous. Med., 1998, 33(1 – 2): 173 – 204.

[11] Greenberg J, Moller N. The prediction of mineral solubilities in natural waters: A chemical equilibrium model for the $Na - K - Ca - Cl - SO_4 - H_2O$ system to high concentration from 0 to 25 ℃ [J]. Geochim. Cosmochim. Acta, 1989, 53(10): 2503 – 2518.

[12] Moller N. The prediction of mineral solubilities in natural waters: A chemical equilibrium model for the $Na - Ca - Cl - SO_4 - H_2O$ system, to high temperature and concentration [J]. Geochim. Cosmochim. Acta, 1988, 52(4): 821 – 837.

[13] Spencer R J, Moller N, Weare J H. The prediction of mineral solubilities in natural waters: A chemical equilibrium model for the system $Na - K - Ca - Cl - SO_4 - H_2O$ at temperatures below 25 ℃ [J]. Geochim. Cosmochim. Acta, 1990, 54(3): 575 – 590.

[14] Song P S. Calculation of the metastable phase diagram for seawater system [J]. J Salt Lake Res, 1998, 6(2 – 3): 17 – 26.

[15] Fang C H, Song P S, Chen J Q. Theoratical calculation of the metastable phase diagram of the quinary system Na^+, K^+ // Cl^-, SO_4^{2-}, CO_3^{2-} – H_2O at 25 ℃ [J]. J. Salt Lake Res., 1993, 1(2): 16 – 22.

[16] Analytical lab of the Qinghai institute of salt lakes at CAS. The Analyses of Brines and Salts [M]. 2nd ed. Beijing: Science Press, 1988.

[17] Harvie C E, Moller N, Weare J H. The prediction in mineral solubilities in natural waters; the $Na - K - Mg - Ca - H - Cl - SO_4 - OH - HCO_3 - CO_3 - CO_2 - H_2O$ system to high ionic strengths at 25 ℃ [J]. Geochim. Cosmochim. Acta, 1980, 48(4): 723 – 751.

[18] Harvie C E, Weare J H. The prediction of mineral solubilities in natural waters: the $Na - K - Mg - Ca - Cl - SO_4 - H_2O$ system from zero to high concentration at 25 ℃ [J]. Geochim. Cosmochim. Acta, 1980, 44(7): 981 – 997.

[19] Pabalan R T, Pitzer K S, Geochim K S. Thermodynamics of concentrated electrolyte mixtures and the prediction of mineral solubilities to high temperatures for mixtures in the system $Na - K - Mg - Cl - SO_4 - OH - H_2O$ [J]. Cosmochim. Acta, 1987, 51(9): 2429 – 2443.

[20] Gibbard H F, Scatchar G. Liquid-vapor equilibrium of aqueous lithium chloride, from 25 to 100 deg. and from 1.0 to 18.5 molal, and related properties [J]. J. Chem. Eng. Data, 1973, 18(3): 293 – 298.

[21] Holmes H F, Mesmer R E. Thermodynamics of aqueous solutions of the alkali metal sulfates [J]. J. Solution. Chem., 1986, 15: 495 – 517.

[22] Skarulis J A, Horan H A. The system $Na_2SO_4 - Li_2SO_4 - H_2O$ at 75 ℃ [J]. J. Am. Chem., Soc., 1955, 77(13): 3489 – 3490.

[23] Akopov E K, Zh. Prikl. Khim, Silcock H. The system $LiCl - NaCl - H_2O$ at 75 ℃ [J]. Solubilities of Inorganic and Organic Compounds, 1963, 36(9): 1916.